

On the stability of bow shocks generated by red supergiants: the case of IRC –10414

D. M.-A. Meyer,^{1*} V. V. Gvaramadze,^{2,3} N. Langer,¹ J. Mackey,¹ P. Boumis,⁴ and S. Mohamed⁵

¹*Argelander-Institut für Astronomie der Universität Bonn, Auf dem Hügel 71, 53121, Bonn, Germany*

²*Sternberg Astronomical Institute, Lomonosov Moscow State University, Universitetskij Pr. 13, Moscow 119992, Russia*

³*Isaac Newton Institute of Chile, Moscow Branch, Universitetskij Pr. 13, Moscow 119992, Russia*

⁴*Institute for Astronomy, Astrophysics, Space Applications and Remote Sensing, National Observatory of Athens, I. Metaxa & Vas. Pavlou St., Palaia Penteli, 15236 Athens, Greece*

⁵*South African Astronomical Observatory, Observatory Road, Observatory, Cape Town, 7925, South Africa*

Accepted 2013 December 05. Received 2013 December 05; in original form 2013 November 18

ABSTRACT

In this Letter, we explore the hypothesis that the smooth appearance of bow shocks around some red supergiants (RSGs) might be caused by the ionization of their winds by external sources of radiation. Our numerical simulations of the bow shock generated by IRC –10414 (the first-ever RSG with an optically detected bow shock) show that the ionization of the wind results in its acceleration by a factor of two, which reduces the difference between the wind and space velocities of the star and makes the contact discontinuity of the bow shock stable for a range of stellar space velocities and mass-loss rates. Our best fit model reproduces the overall shape and surface brightness of the observed bow shock and suggests that the space velocity and mass-loss rate of IRC –10414 are $\approx 50 \text{ km s}^{-1}$ and $\approx 10^{-6} \text{ M}_{\odot} \text{ yr}^{-1}$, respectively, and that the number density of the local ISM is $\approx 3 \text{ cm}^{-3}$. It also shows that the bow shock emission comes mainly from the shocked stellar wind. This naturally explains the enhanced nitrogen abundance in the line-emitting material, derived from the spectroscopy of the bow shock. We found that photoionized bow shocks are $\approx 15\text{--}50$ times brighter in optical line emission than their neutral counterparts, from which we conclude that the bow shock of IRC –10414 must be photoionized.

Key words: methods: numerical – shock waves - circumstellar matter - stars: individual: IRC –10414 – stars: massive.

1 INTRODUCTION

A significant fraction of runaway OB stars are moving supersonically through the local interstellar medium (ISM) (Huthoff & Kaper 2002) and therefore generate bow shocks. The detection of these arc-like structures serves as an indication that their associated stars are massive enough to possess strong winds and could be used for i) identifying distant and/or highly reddened (runaway) OB stars (e.g. Gvaramadze, Kroupa & Pflamm-Altenburg 2010), ii) searching for parent clusters to these stars (e.g. Gvaramadze & Bomans 2008) and iii) constraining their mass-loss rates (Kobulnicky, Gilbert & Kiminki 2010; Gvaramadze, Langer & Mackey 2012) and parameters of the local ISM (Kaper et al. 1997; Gvaramadze et al. 2013, hereafter Paper I).

Analytical (Dgani, van Buren & Noriega-Crespo 1996)

and numerical studies (Comerón & Kaper 1998; Blondin & Koerwer 1998) of bow shocks show that they are subject to different kinds of instabilities, which along with density inhomogeneities and interstellar magnetic field can significantly affect their appearance. In particular, Dgani et al. (1996) showed that isothermal bow shocks are unstable if the stellar space velocity, v_* , is larger than the wind velocity, v_w . This condition is usually fulfilled by cool runaway stars, e.g., red supergiants (RSGs), whose wind velocities of $\approx 20 \text{ km s}^{-1}$ are comparable to or less than their typical space velocities of several tens of km s^{-1} . Numerical simulations of bow shocks produced by RSGs (Brighenti & D’Ercole 1995; Mohamed, Mackey & Langer 2012; Cox et al. 2012; Decin et al. 2012) confirmed that they are indeed generally unstable to a significant degree. This result is in conflict with the observed smoothness of bow shocks associated with two of the three known bow-shock-producing RSGs, namely Betelgeuse (Noriega-Crespo et al. 1997) and IRC –10414 (Pa-

* E-mail: dmeyer@astro.uni-bonn.de

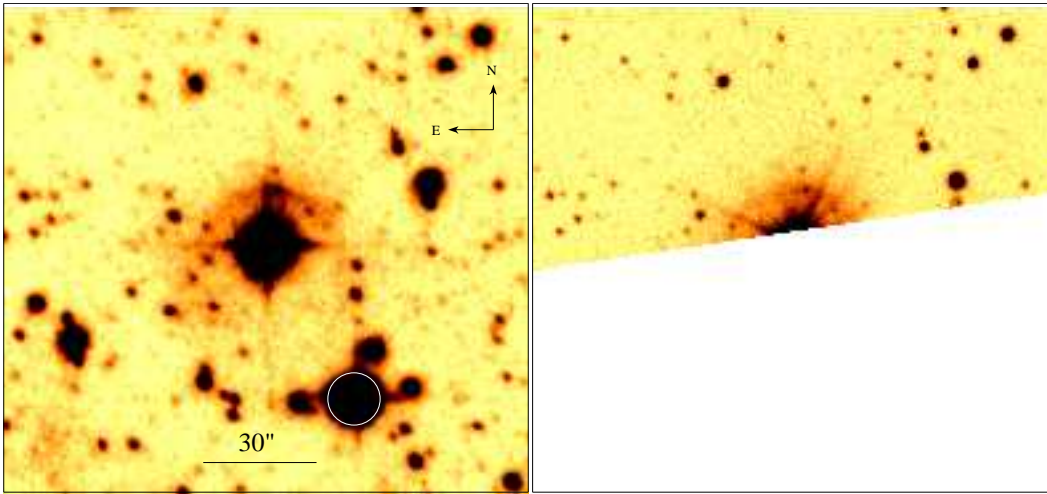


Figure 1. Left: $H\alpha+[NII]$ image of IRC –10414 and its bow shock from the SHS. The WC5 star WR 114, located at ≈ 45 arcsec southwest of IRC –10414, is marked by a white circle. Right: $H\alpha+[NII]$ image of the bow shock obtained with the 2.3-m Aristarchos telescope (the image is truncated because the CCD detector was offset from IRC –10414 to avoid saturation). The orientation and the scale of the images are the same. See the text for details. At a distance of 2 kpc, 30 arcsec correspond to ≈ 0.29 pc.

per I). On the other hand, a bow shock around the third of these RSGs, μ Cep, shows clear signatures of instabilities (Cox et al. 2012) in good agreement with the theoretical and numerical predictions. There should therefore exist some factors which stabilize bow shocks around RSGs. Decin et al. (2012) began to explore this subject by considering a bow shock from a RSG with a neutral wind but moving in an ionized ISM (photoheated to 8000 K), finding that this reduced the strength of instabilities compared to a bow shock in a neutral ISM.

In this Letter, we use numerical simulations of the bow shock of IRC –10414 to investigate the hypothesis that bow shocks generated by RSGs could be stable if the stellar wind and the ambient ISM are heated and ionized by an external source of radiation. The relevant data on the bow shock are reviewed in Section 2. The numerical models of the bow shock are presented in Section 3 and discussed in Section 4. We summarize in Section 5.

2 THE BOW SHOCK OF IRC –10414

The bow shock around IRC –10414 is the first-ever optically detected bow shock generated by RSGs (the data on the bow shock and IRC –10414 quoted below are from Paper I unless otherwise stated). The left-hand panel of Fig. 1 presents the discovery $H\alpha+[NII]$ $\lambda\lambda 6548, 6584$ image of the bow shock from the SuperCOSMOS H-alpha Survey (SHS; Parker et al. 2005), showing a smooth arc-like nebula at ≈ 15 arcsec from the star. At a distance to IRC –10414 of 2 kpc (Maeda et al. 2008), the stand-off distance of the bow shock is $R_{SO} \approx 0.14$ pc. For an inclination angle of the bow shock to the plane of the sky of $\approx 20^\circ$, the projection effect on the observed R_{SO} is negligible (see Gvaramadze et al. 2011). The right-hand panel of Fig. 1 shows a follow-up image of the bow shock obtained with the 2.3-m Aristarchos f/8 telescope at Helmos Observatory, Greece on 2013 August 9 with 1800 s exposure, through a 40 \AA bandwidth filter centred on the $H\alpha+[NII]$ lines. To avoid saturation, IRC –10414 was placed outside

the CCD detector. Although the resolution of this image is about three times higher than that of the SHS one, the bow shock still does not show any signatures of instabilities.

Using equation (1) and the flux calibration factor of $16.1 \text{ counts pixel}^{-1} R^{-1}$ from Table 1 in Frew et al. (2013), we derived from the SHS image the surface brightness of the bow shock near the apex of $\Sigma_{obs} \approx 77 R$ ($1R \equiv 1 \text{ Rayleigh} = 5.66 \times 10^{-18} \text{ erg cm}^{-2} \text{ s}^{-1} \text{ arcsec}^{-2}$ at $H\alpha$).

Optical spectroscopy of the bow shock (carried out with the Southern African Large Telescope) showed that the line-emitting material is enriched in nitrogen, which implies that the emission at least partially originates from the shocked stellar wind (cf. Section 4). It also allowed us to constrain the number density of the ambient ISM to be $n_0 \leq 5 \text{ cm}^{-3} (v_*/70 \text{ km s}^{-1})^{-2}$ (see Paper I for details), which in its turn imposes a limitation on the mass-loss rate, \dot{M} , of IRC –10414. The space velocity of IRC –10414 $v_* \approx 70 \pm 20 \text{ km s}^{-1}$ is several times higher than the stellar wind velocity $v_w = 21 \pm 2 \text{ km s}^{-1}$, derived from maser observations of a region within a few hundreds of AU from the star. Thus, if the bow shock of IRC –10414 is a thin shell (a natural assumption for bow shocks produced by cool stars), then, according to Dgani et al. (1996), it should be unstable and ragged, which clearly contradicts our observations.

Previous numerical simulations of bow shocks generated by RSGs proceeded from the common assumption that the stellar wind is neutral. This assumption, however, would be invalidated if the wind is ionized by an external source of radiation, like a nearby hot massive star or a star cluster. Good examples of such situation are ionized nebulae around the RSGs NML Cyg and W26, which are the result of ionization of the stellar wind by the nearby association Cyg OB2 (Morris & Jura 1983) and star cluster Westerlund 1 (Wright et al. 2013), respectively. As discussed in Paper I, the ionization of the wind might exert a stabilizing influence on RSG bow shocks. Proceeding from this, we proposed that the smooth shape of the bow shock around IRC –10414 is because the wind of this star and the ambient ISM are ionized by the nearby WC5 star WR 114 (see Fig. 1) and/or by the massive

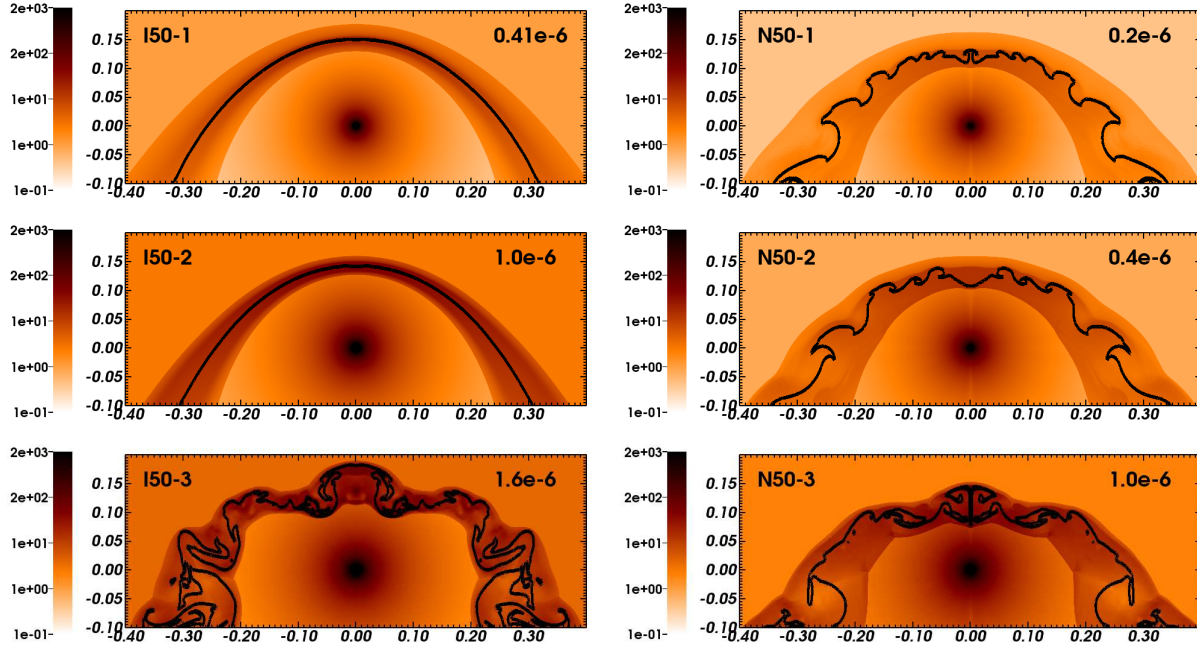


Figure 2. Grid of models of the bow shock generated by a RSG moving at 50 km s^{-1} . The panels show the gas number density plotted on the logarithmic scale in units of cm^{-3} . The left-hand panels present the fully ionized models and the right-hand panels the neutral ones. On each panel the left-hand key refers to the nomenclature detailed in Table 1 and the right-hand key indicates \dot{M} in units of $M_{\odot} \text{ yr}^{-1}$. The solid line traces the position of the contact discontinuity. Models are shown at least 0.1 Myr after the beginning of the simulations. The x -axis corresponds to the radial direction and the symmetry axis is aligned with the space velocity of the star (both axes are in units of pc). Note that not all of the computational domain is shown.

Table 1. Input parameters of the grid models and the surface brightness of the model bow shocks. Columns show, respectively, model identifier, space velocity in km s^{-1} , mass-loss rate in $10^{-6} M_{\odot} \text{ yr}^{-1}$, ambient ISM number density in cm^{-3} , and maximum surface brightness of the models, before and after correction for the interstellar extinction towards IRC -10414 , in Rayleighs.

Model	v_*	\dot{M}	n_0	Σ_{max}	$\Sigma_{\text{max}}^{\text{cor}}$
I50-1	50	0.41	1.21	133.2	5.3
I50-2	50	1.01	3.30	1176.7	47.1
I50-3	50	1.62	5.00	8436.8	337.5
I70-1	70	0.41	0.73	155.4	6.2
I70-2	70	1.01	1.51	865.9	34.6
I90-1	90	0.41	0.41	144.3	5.8
N50-1	50	0.20	0.48	3.1	0.1
N50-2	50	0.41	0.91	8.0	0.3
N50-3	50	1.01	2.60	33.3	1.3
N70-1	70	0.41	0.35	3.1	0.1
N90-1	90	0.41	0.26	9.5	0.4

star cluster NGC 6611. In this connection, we note that the spectrum of the bow shock shows very strong [N II] $\lambda\lambda 6548, 6583$ emission lines (see fig. 3 in Paper I), which means that the stellar wind is ionized to a significant degree (cf. Section 4). Since the wind material cannot be collisionally ionized because the reverse shock is too weak, it is natural to assume that the wind is photoionized by an external source. The above considerations motivated us to carry out numerical simulations presented in this Letter.

3 NUMERICAL SIMULATIONS

We performed 2D numerical simulations using the PLUTO code (Mignone et al. 2007, 2012). The simulations were carried out in cylindrical coordinates on a uniform grid of size $[0, 0.4] \times [-0.1, 0.3]$ pc and spatial resolution of $2.25 \times 10^{-4} \text{ pc cell}^{-1}$. A stellar wind was injected into the computational domain via a half circle of radius of 20 cells ($\approx 900 \text{ AU}$) centred at the origin, and its interaction with the ISM was modelled in the reference frame of the star. Wind material is distinguished from the ISM using a passive tracer advected together with the fluid. The ISM composition is assumed to be solar (Asplund et al. 2009).

Optically-thin radiative cooling and heating were taken into account. For a fully ionized medium, the cooling curve is the sum of contributions from H, He and metals (Wiersma, Schaye & Smith 2009), collisionally excited forbidden lines (Henney et al. 2009) and H recombination together with heating from the reionization of recombining H atoms (Osterbrock & Bochkarev 1989; Hummer 1994). The equilibrium temperature of this curve is $\approx 8000 \text{ K}$. For models with the neutral medium, the cooling curve is the sum of contributions from H, He and metals (Wiersma et al. 2009) and the dust heating by the Galactic far-ultraviolet background (Wolfire et al. 2003). The equilibrium temperature of this curve is $\approx 3300 \text{ K}$ for $n_0 = 1 \text{ cm}^{-3}$. All models include electronic thermal conduction (Cowie & McKee 1977).

We have run a grid of 11 models, in which both the stellar wind and the ISM were considered to be either fully ionized or neutral, labelled ‘I’ and ‘N’, respectively. Three space velocities were considered, $v_* = 50, 70$ and 90 km s^{-1} , and $v_w = 21 \text{ km s}^{-1}$ was set in all models. For \dot{M} we adopted

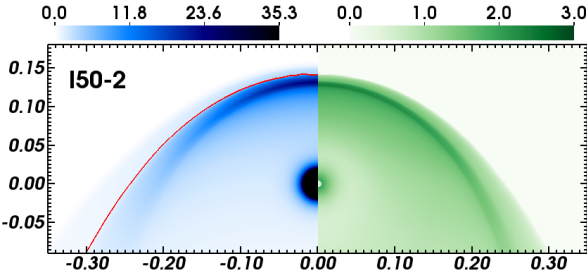


Figure 3. Left: Surface brightness for the ionized model I50-2 plotted on a linear scale in units of R . The solid (red) line traces the position of the contact discontinuity. Right: $[\text{NII}]/\text{H}\alpha$ line ratio for the same model.

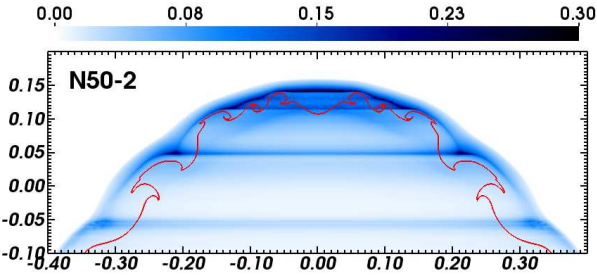


Figure 4. Surface brightness for the neutral model N50-2 plotted on a linear scale in units of R . The solid (red) line traces the position of the contact discontinuity

a range of values based on various mass-loss prescriptions proposed for RSGs (see Paper I), ranging from $\approx 0.4 \times 10^{-6}$ to $1.6 \times 10^{-6} M_{\odot} \text{ yr}^{-1}$. For each model, n_0 was adjusted in such a way that R_{SO} of a model bow shock is equal to the observed one, when a steady state was reached. All models are run for at least 0.1 Myr, which corresponds to more than 16 grid crossing times. The parameters of the models are summarized in Table 1.

For the sake of comparison with observations, we calculated the $\text{H}\alpha + [\text{NII}]$ surface brightness of the model bow shocks using the prescriptions by Dopita (1973) and Osterbrock & Bochkarev (1989). To reproduce the observed $[\text{NII}]/\text{H}\alpha$ line ratio of 2.4 ± 0.1 (measured in the spectrum of the bow shock at an angle of 25° from the apex; see Paper I), we assumed that the RSG wind is enriched in nitrogen by a factor of 6 (cf. Brott et al. 2011). The maximum value of the brightness, Σ_{max} , for each model is given in the column 5 of Table 1, while the column 6 gives Σ_{max} corrected for the interstellar extinction towards IRC –10414, which in the R -band is ≈ 3.5 mag (Paper I).

4 RESULTS AND DISCUSSION

Fig. 2 plots the gas number density of the ionized (left-hand panels) and neutral bow shocks generated by RSGs moving with a velocity of 50 km s^{-1} . The solid (black) line traces the position of the contact discontinuity. One can see that the ionized bow shocks are stable as long as $\dot{M} \lesssim 1 \times 10^{-6}$

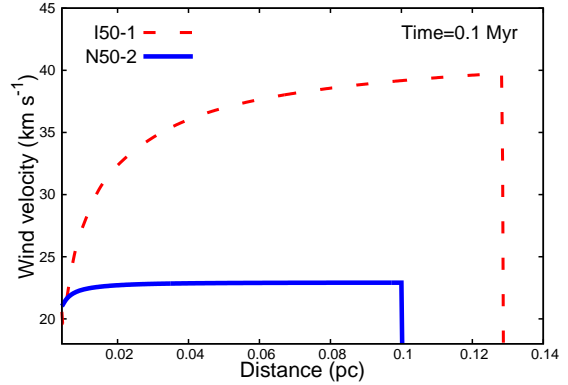


Figure 5. Wind velocity profiles along the y -axis for the models I50-1 and N50-2. Heating of the wind by photoionization results in its acceleration by a factor of two (see the text for details).

$M_{\odot} \text{ yr}^{-1}$. For higher \dot{M} and/or v_* , the ionized bow shocks became unstable (e.g. model I50-3 in Fig. 2), which prevent them from reaching a steady state. Of three neutral models shown in Fig. 2 two ones have smooth forward and reverse shocks, while the contact discontinuity in all of them is very ragged. For $\dot{M} \gtrsim 10^{-6} M_{\odot} \text{ yr}^{-1}$ and/or $v_* > 50 \text{ km s}^{-1}$, the contact discontinuity becomes even more unstable and the overall shape of the neutral bow shocks becomes highly distorted (e.g. model N50-3 in Fig. 2). We therefore expect that one of the models I50-1, I50-2, N50-1 and N50-2 could represent the bow shock around IRC –10414.

To substantiate this expectation, we compare Σ_{obs} with the model predictions. An inspection of Table 1 shows that the higher \dot{M} the higher Σ_{max} of the models. Three of the ionized models have $\Sigma_{\text{max}}^{\text{cor}}$ comparable to or larger than Σ_{obs} . Of these models only I50-2 is stable (see Fig. 2). $\Sigma_{\text{max}}^{\text{cor}}$ of the remaining three ionized models slightly exceeds the sensitivity limit to diffuse emission of the SHS of 2–5 R (Parker et al. 2005) and therefore, in principle, these bow shocks could be detected with this survey. On the contrary, all the neutral models are so dim that their $\Sigma_{\text{max}}^{\text{cor}}$ is below the sensitivity limit of the SHS. Thus, we conclude that I50-2 is the best fit model of the bow shock of IRC –10414. Interestingly, \dot{M} adopted in this model is a factor of 5–10 smaller than that predicted by most of the mass-loss prescriptions proposed for RSGs (see Paper I) and a factor of two higher than what follows from the recipe by Verhoelst et al. (2009).

The left-hand panel of Fig. 3 presents a map of the surface brightness in the $\text{H}\alpha + [\text{NII}]$ lines for our preferred model I50-2. It shows that the emission comes mainly from the shocked wind, which naturally explains why the brightness of the ionized models increases with \dot{M} (see Table 1) and why the line-emitting material in the bow shock of IRC –10414 is enriched in nitrogen. The right-hand panel of Fig. 3 plots the $[\text{NII}]/\text{H}\alpha$ line ratio for the emission originating from the shocked wind for the same model. This ratio has a value of 2.3 for an angle of 25° from the apex of the bow shock, which is in a good agreement with the observed value of 2.4 ± 0.1 .

Fig. 4 plots the surface brightness for the neutral model N50-2. Unlike the ionized models, the $\text{H}\alpha + [\text{NII}]$ emission in the neutral ones originates from the collisionally ionized ISM, i.e. just behind the forward shock. Correspondingly, the model N50-2 has a rather smooth appearance, but its $\Sigma_{\text{max}}^{\text{cor}}$ is below the sensitivity limit of the SHS. This further

supports our claim that the bow shock of IRC−10414 is ionized by an external source.

Using Fig. 3, we measured a ratio $R_{\text{SO}}/R(\theta)$, where $R(\theta)$ is the distance between the star and the bow shock at an angle θ from the apex. For $\theta \approx 75^\circ$ (the half-opening angle of the observed bow shock), we found $R_{\text{SO}}/R(\theta) = 1.36$, which is in a reasonable agreement with both the observed ratio of 1.33 and the theoretical one of 1.44, derived from the thin-shell bow shock model by Wilkin (1996).

It should be noted that the ionized models have higher ISM densities than the neutral ones with the same v_* and \dot{M} (see Table 1). Since R_{SO} is fixed in all models, this difference implies that the wind velocity is higher in the ionized models. Indeed, the instantaneous heating of the wind material up to ≈ 8000 K results in increase of its thermal pressure, which in its turn leads to the wind acceleration (see Oort & Spitzer 1955 for more details). Fig. 5 shows the wind velocity profiles along the y -axis for the models I50-1 and N50-2. In I50-1 the wind is accelerated by a factor of two and its velocity becomes comparable to v_* , while in N50-2 the wind velocity remains constant¹, i.e. a factor of ≈ 2.5 less than v_* . Correspondingly, the shear produced by the relative motion of the shocked wind and shocked ISM is stronger in the N50-2 model, which makes it more prone to the development of the Kelvin-Helmholtz instability at the contact discontinuity. The same is true for the models with higher v_* because the growth time of the instability is inversely proportional to the magnitude of the shear, which in its turn increases with v_* .

5 SUMMARY

In this Letter, we presented a grid of models of bow shocks produced by RSGs, in which both the stellar wind and the ISM were considered to be either fully ionized or neutral. We investigated whether the smooth appearance of the bow shock around the RSG IRC−10414 might be caused by the ionization of the stellar wind by an external source of radiation. We found that although both kinds of models can have a smooth appearance in the $\text{H}\alpha + [\text{N II}]$ lines, only the ionized ones can simultaneously reproduce the overall shape and the brightness of this bow shock. Our simulations showed that the ionization of the stellar wind results in its acceleration by a factor of two, which reduces the shear at the contact discontinuity and makes the bow shock stable for a range of stellar space velocities and mass-loss rates. Our best fit model of the bow shock suggests that the space velocity and mass-loss rate of IRC−10414 are $\approx 50 \text{ km s}^{-1}$ and $\approx 10^{-6} M_\odot \text{ yr}^{-1}$, respectively, and that the number density of the local ISM is $\approx 3 \text{ cm}^{-3}$. We found also that in the ionized models the $\text{H}\alpha + [\text{N II}]$ emission originates mostly from the shocked RSG wind, which naturally explains why the line-emitting material in the bow shock of IRC−10414 is enriched in nitrogen. Our results suggest that the ionization of the stellar wind might be responsible for the smooth appearance of bow shocks generated by other RSGs, or asymptotic giant branch stars.

¹ A slight acceleration of the wind in this model is because of a boundary effect.

6 ACKNOWLEDGEMENTS

We are grateful to D.J. Frew for providing us with data before publication. JM acknowledges funding from the Alexander von Humboldt Foundation and the Deutsche Forschungsgemeinschaft priority program 1573, ‘Physics of the Interstellar Medium’. The Aristarchos telescope is operated on Helmos Observatory by the Institute of Astronomy, Astrophysics, Space Applications and Remote Sensing of the National Observatory of Athens. All the simulations were run on the JUROPA supercomputer at the Jülich Supercomputing Centre.

REFERENCES

- Asplund M., Grevesse N., Sauval A. J., Scott P., 2009, *ARA&A*, 47, 481
- Blondin J.M., Koerwer J.F., 1998, *NewA*, 3, 571
- Brighenti F., D’Ercole A., 1995, *MNRAS*, 277, 53
- Brott I. et al., 2011, *A&A*, 530, A115
- Comerón F., Kaper L., 1998, *A&A*, 338, 273
- Cowie L.L., McKee C.F., 1977, *ApJ*, 211, 135
- Cox N.L.J. et al., 2012, *A&A*, 537, A35
- Decin L. et al., 2012, *A&A*, 548, A113
- Dgani R., van Buren D., Noriega-Crespo A., 1996, *ApJ*, 461, 927
- Dopita M.A., 1973, *A&A*, 29, 387
- Frew D.J., Bojčić I.S., Parker Q.A., Pierce M.J., Gunawardhana M.L.P., Reid W.A., 2013, *MNRAS*, in press (arXiv:1303.4555)
- Gvaramadze V.V., Bomans D.J., 2008, *A&A*, 490, 1071
- Gvaramadze V.V., Kroupa P., Pflamm-Altenburg J., 2010, *A&A*, 519, A33
- Gvaramadze V.V., Langer N., Mackey J., 2012, *MNRAS*, 427, L50
- Gvaramadze V.V., Röser S., Scholz R.-D., Schilbach E., 2011, *A&A*, 529, A14
- Gvaramadze V.V., Menten K.M., Kniazev A.Y., Langer N., Mackey J., Kraus A., Meyer D.M.-A., Kaminski T., 2013, *MNRAS*, in press (arXiv:1310.2245) (Paper I)
- Henney W.J., Arthur S.J., de Colle F., Mellema G., 2009, *MNRAS*, 398, 157
- Hummer D.G., 1994, *MNRAS*, 268, 109
- Huthoff F., Kaper L., 2002, *A&A*, 383, 999
- Kaper L., van Loon J.Th., Augusteyn T., Goudfrooij P., Patat F., Waters L.B.F.M., Zijlstra A.A., 1997, *ApJ*, 475, L37
- Kobulnicky H.A., Gilbert I.J., Kiminki D.C., 2010, *ApJ*, 710, 549
- Maeda T. et al., 2008, *PASJ*, 60, 1057
- Mignone A., Bodo G., Massaglia S., Matsakos T., Tesileanu O., Zanni C., Ferrari A., 2007, *ApJS*, 170, 228
- Mignone A., Zanni C., Tzeferacos P., van Straalen B., Colella P., Bodo G., 2012, *ApJS*, 198, 7
- Mohamed S., Mackey J., Langer N., 2012, *A&A*, 541, A1
- Morris M., Jura M., 1983, *ApJ*, 267, 179
- Noriega-Crespo A., van Buren D., Cao Y., Dgani R., 1997, *AJ*, 114, 837
- Oort J.H., Spitzer L.Jr, 1955, *ApJ*, 121, 6
- Osterbrock D.E., Bochkarev N.G., 1989, *Soviet Ast.*, 33, 694
- Parker Q.A. et al., 2005, *MNRAS*, 362, 689
- Verhoelst T., Van der Zypen N., Hony S., Decin L., Cami J., Eriksson K., 2009, *A&A*, 498, 127
- Wiersma R.P.C., Schaye J., Smith B.D., 2009, *MNRAS*, 393, 99
- Wilkin F., 1996, *ApJ*, 459, 31
- Wolfire M.G., McKee C.F., Hollenbach D., Tielens A.G.G.M., 2003, *ApJ*, 587, 278
- Wright N.J. et al., 2013, *MNRAS*, in press (arXiv:1309.4086)